Chinese Chemical Letters 34 (2023) 107684

Contents lists available at ScienceDirect

Chinese Chemical Letters

journal homepage: www.elsevier.com/locate/cclet

Hydrogen bonding-induced oxygen clusters and long-lived room temperature phosphorescence from amorphous polyols

Ya-Ling Wang[a,1], Kang Chen[b,1], Hai-Ru Li[a], Bo Chu[c], Zishan Yan[b], Hao-Ke Zhang[c], Bin Liu[a,*], Shengliang Hu[a], Yongzhen Yang[b,d,*]

[a] School of Energy and Power Engineering, North University of China, Taiyuan 030051, China
[b] MOE Key Laboratory of Interface Science and Engineering in Advanced Materials, Taiyuan University of Technology, Taiyuan 030024, China
[c] Department of Polymer Science and Engineering, MOE Key Laboratory of Macromolecular Synthesis and Functionalization, Zhejiang University, Hangzhou 310027, China
[d] Shanxi-Zheda Institute of Advanced Materials and Chemical Engineering, Taiyuan 030032, China

ARTICLE INFO

Article history:
Received 5 July 2022
Revised 7 July 2022
Accepted 15 July 2022
Available online 17 July 2022

Keywords:
Clusteroluminescence
Through-space interactions
Polymethylol
Poly(3-butene-1,2-diol)
Hydrogen bonding
Polymerization

ABSTRACT

Developing non-conjugated luminescent polymers (NCLPs) with fluorescence and long-lived room-temperature phosphorescence is of great significance for revealing the essence of NCLPs luminescence, which has gradually attracted the attention of researchers in recent years. Herein, polymethylol (PMO) and poly(3-butene-1,2-diol) (PBD) with polyhydroxy structures were prepared and their luminescence behaviors were investigated to reveal the clusteroluminescence (CL) mechanism. Compared with polyvinyl alcohol with non-luminescent behavior, PMO and PBD exhibit cyan-blue fluorescence with quantum yields of *ca.* 12% and green room-temperature phosphorescence with lifetimes of *ca.* 89 ms in the solid state. Both fluorescence and phosphorescence exhibit typical excitation-dependent CL behavior. Experimental and theoretical analyses show that the strong hydrogen-bonding interaction of PMO and PBD greatly promotes the formation of oxygen clusters and the through-space n-n interaction of oxygen atoms, enabling fluorescence and phosphorescence emission. Our results have enormous implications for understanding the CL mechanism of NCLPs and provide a new polymer design strategy for the rational design of novel NCLPs materials.

Light is an essential factor for human survival, health, and development. Thereinto, fluorescence and phosphorescence play a vital role in optoelectronic devices [1], chemo-/bioprobes [2,3], biological imaging [4,5], and other fields [6,7]. Conventional wisdom holds that chromophores with well-defined large conjugated groups are required to achieve fluorescence or/and phosphorescence emission [8,9]. However, in recent years, numerous studies have found that many natural and synthetic polymers or small molecules, in the absence of well-defined chromophores or conjugated structures, also exhibit fluorescence or/and even room temperature phosphorescence (RTP), such as polyether [10], polyester [11,12], natural products [13], poly(maleic anhydride) derivatives [14–17], tertiary amine derivatives [18,19], poly(hydroxyurethane) [20] and polysiloxane [21]. The structures of these molecules usually contain heteroatom groups (such as N, O, S), and their luminescence exhibits concentration-dependent, solid-state fluorescence, and excitation-dependent emission, belonging to typical clusterization-triggered emission (CTE) or clusteroluminescence (CL) [22,23]. The classical through-bond conjugation theory is difficult to explain such non-conjugated luminescence molecules. In this case, CTE or CL has been widely recognized and concerned by researchers since it was proposed [14,24]. However, owing to the inclusion of both n and π electrons in the molecular structure, the intrinsic CL mechanism remains obscure, although it has been tentatively uncovered in previous works [10,12,25,26]. Therefore, it is urgent to construct a class of typical luminescent model molecules with simple and well-defined structures to further clarify the CL mechanism.

Phosphorescence is another aspect and channel to reveal the CL mechanism. But for spin-forbidden phosphorescence, the vibration and rotation of molecules and the effects of external conditions (such as oxygen and moisture) greatly limit the generation of phosphorescence, especially for RTP. Facilitating the singlet-to-triplet intersystem crossing (ISC) to populate the triplet and stabilizing the triplet excitons to inhibit the nonradiative transition pathways

* Corresponding authors.
E-mail addresses: liubin@nuc.edu.cn (B. Liu), yyztyut@126.com (Y. Yang).
[1] These authors contributed equally to this work.

https://doi.org/10.1016/j.cclet.2022.07.027
1001-8417/

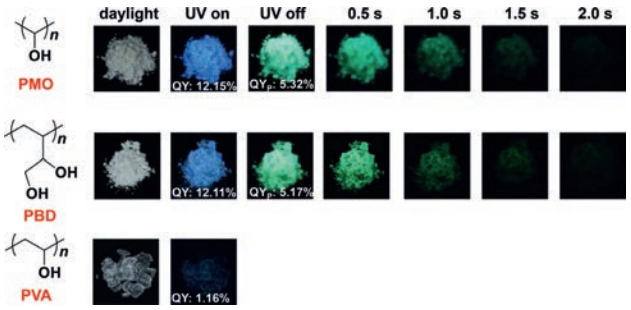

Fig. 1. Structures and photographs of PMO, PVA and PBD taken in daylight, before and after ceasing the 365 nm UV irradiation.

are key principles to achieve phosphorescence emission. The phenomenon of RTP has long been synonymous with metallic and inorganic complexes [27,28]. Nonetheless, over the past few years, purely organic luminophores have gradually been endowed with long-lived RTP through precise molecular design. The main strategies to achieve its RTP are the introduction of heavy atoms (*e.g.*, halogens) [29], crystallization [30,31], and host-guest interactions [32]. Among them, crystallization is an effective and commonly used approach to achieve RTP emission because it can induce intramolecular motion restriction to produce rigid molecular conformations, ultimately inhibiting nonradiative decay [10,25,33]. However, the crystallinity of polymers tends to vary greatly depending on post-processing methods, which affects the emission intensity and lifetime of their RTPs, restricting their specific practical applications. Instead, hydrogen bonding (H-bonding) is a crystallization-like strategy that can be readily constructed in amorphous polymers to achieve conformational rigidification. Also, many RTP systems also select polymers with multiple H-bonding as matrix, *e.g.*, polyvinyl alcohol (PVA) [34]. However, developing amorphous RTP non-conjugated luminescent polymers (NCLPs) and revealing their luminescence mechanism remains a challenge.

In this work, polymethylol (PMO) and poly(3-butene-1,2-diol) (PBD) with one hydroxyl group on each carbon atom in the backbone and side chain were designed and synthesized, and their luminescence properties were studied in detail to understand the CL mechanism. The extremely strong H-bonding of PMO and PBD induces the generation of oxygen clusters and through-space n-n interactions of oxygen atoms, which is the source of the strong fluorescence and long-lived RTP. Theoretical analysis shows that the distance among a large number of oxygen atoms ranges in 2.58−2.83 Å, which is less than twice the van der Waals radius of oxygen atom (r_B: 1.52 Å; r_P: 1.40 Å). The existence of oxygen clusters and through-space n-n interactions are confirmed. The above results also fully demonstrate that even without crystallization and π electrons, CL can be realized through the action of H-bonding. And if the H-bonding is strong enough, nonradiative decays can be suppressed to produce RTP.

As a well-known polymer with a polyhydroxyl structure, PVA possesses one dissociative −OH group on every two carbon atoms in the backbone. In contrast to PVA, PMO and PBD have one −OH group on each carbon atom in the backbone and side chain (Fig. 1), which makes it necessary to consider strong H-bonding in the study of photophysical properties. In order to synthesize PMO and PBD, poly(vinylene carbonate) (PVC) and poly(vinylethylene carbonate) (PVEC) were firstly prepared by the radical polymerization of vinylene carbonate and vinylethylene carbonate using 2,2′-azobisisobutyronitrile (AIBN) as a radical initiator, respectively (Schemes S1 and S2 in Supporting information) [35–37]. The proton nuclear magnetic resonance spectroscopy (^{1}H NMR) and gel permeation chromatography (GPC) data indicated that PVC and PVEC were successfully synthesized (Figs. S1-S4 in Supporting information). The number-averaged molecular weights (M_n) and polydispersity indexs (PDI) were 102.8 kg/mol, 1.4 for PVC and 52.1 kg/mol, 1.2 for PVEC, respectively. Then, PVC and PVEC were hydrolyzed in strong alkaline solution to obtain pure white PMO and PBD powers according to the reported literatures (Fig. 1, Schemes S1 and S2) [38,39]. Fourier transform infrared (FT-IR) spectra show that the C=O stretching vibrations of the five-membered cyclic carbonate of PVC and PVEC at *ca.* 1800 cm^{-1} disappears completely, proving the successful synthesis of PMO and PBD (Figs. S5 and S6 in Supporting information). Also, compared with the sharp stretching vibration peak of free −OH group located at ∼3600 cm^{-1}, the broad and blue-shifted peak of −OH group indicates the presence of strong H-bonding interactions, which is further confirmed by theoretical calculation (see calculation section in Supporting information for detailed analysis). The glass transition temperatures (T_gs) of PMO and PBD reach 183.3 °C and 113 °C, respectively, indicating amorphous rather than crystalline states (Figs. S7 and S8 in Supporting information). However, owing to the extremely strong H-bonding, they cannot be dissolved in any solvent [40], which extremely limits the study of optical behaviors in solution.

As shown in the structures of Fig. 1, there are no other heteroatoms and π electrons in PMO and PBD except oxygen atoms and n and σ electrons. Nonetheless, both PMO and PBD powders exhibited cyan-blue fluorescence and long-lived green RTP with a duration of 2.0 s, which belongs to the typical CL chromophores. To reveal the CL mechanism, PVA showing very weak fluorescence was chosen as a control owing to the similarity in molecule structure. The photoluminescence/phosphorescence quantum yield (QY/QY$_p$) of PMO and PBD are 12.15%/5.32% and 12.11%/5.17%, (Figs. S9 and S10 in Supporting information) respectively, which are relatively respectable values in NCLPs with RTP, especially for some NCLP systems with only oxygen atoms [10,13,41,42]. Considering that PMO and PBD have similar optical properties, here the PMO is taken as an example for detailed description. The pure white PMO powder shows distinct excitation-dependent photoluminescence (PL) properties (Fig. 2a), similar to many of CL chromophores reported before [22,23,43]. The spectra covered an emission band from 350 to 600 nm, with an emission peak of 438 nm excited by 360 nm (Fig. 2a). The fluorescence lifetime measured at the emission peak of 438 nm was 3.95 ns (Fig. 2b). Theoretically, there's no fluorescence in PMO because there is no definite conjugation unit in the molecular structure of PMO based on the theory of through-bond conjugation [44]. Although the presence of oxygen atoms results in n-σ^* electronic transitions, the energy gap of the (n, σ^*) transition is too high to emit visible light. For example, the energy gap of (n, σ^*) transitions of methanol is around 6.7 eV [45], corresponding to light with a wavelength of 183 nm. Also, the transitions are related to the promotion of an electron from a non-bonding n orbital to σ^* antibonding orbital, which are forbidden transitions and weak intensity. Therefore, the fluorescence of PMO does not originate from the (n, σ^*) transition of oxygen atom. So, what is the origin of such unusual PL? Tang and Yuan *et al.* [22-24,46] proposed the CTE mechanism and through-space interaction (TSI) from isolated aromatic rings and heteroatoms with lone-pair electrons can rationally reveal the PL origin of NCLPs. In this case, the only possibility is that the fluorescence originates from the through-space n-n interaction of oxygen. Owing to the overlap of n electrons of oxygen atoms in PMO, new orbitals with lower HOMO-LUMO gaps from oxygen clusters can be generated compared to single oxygen atoms, which can absorb and emit lower-energy (longer-wavelength) light. Furthermore, differences in TSI degree lead to the emergence of different HOMO-LUMO gaps from diverse oxygen clusters, thus exhibiting excitation-dependent emission characteristics. Meanwhile, the green RTP emission with a maximum emission peak at 500 nm and a lifetime of 89.17 ms was

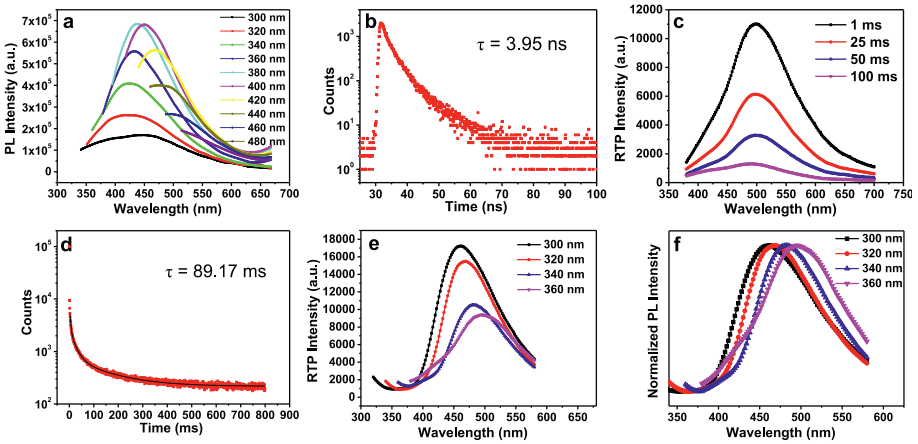

Fig. 2. (a) PL spectra of PMO at different excitation wavelengths in the solid state. (b) Luminescent decay curve of PMO in the solid state at 438 nm (λ_{ex} = 360 nm). (c) Time-resolved spectra of PMO at different delay times in the solid state (phosphorescence mode: λ_{ex} = 360 nm). (d) Phosphorescence decay curve of PMO in the solid state at 500 nm (λ_{ex} = 360 nm). (e) Time-resolved spectra of PMO at different excitation wavelengths in the solid state (delay time: 1 ms). (f) Normalized time-resolved spectra of PMO at different excitation wavelengths in the solid state.

observed (Figs. 2c and d), which is comparable to some crystalline small molecules [47,48]. Similar to the steady-state PL spectra, the phosphorescence spectra also show excitation-dependent emission in the range of 462–500 nm at excitation wavelengths from 300 to 360 nm (Figs. 2e and f). This further confirms the existence of diverse oxygen clusters with different conjugation degrees. And the excitation-dependent emission provides an efficient method to realize multicolor fluorescence and RTP emission.

For such long-lived RTP emission, polymerization and extremely strong H-bonding play a key role. As reported in our previous work [49], polymerization is a very efficient method to achieve PL and RTP emission, namely polymerization-induced emission [50–52]. When the degree of polymerization (DP) of the PMO is 1, 2 or 3, *i.e.*, methanol, ethylene glycol, and glycerol, they emit no PL and RTP as we all known (Figs. S11-S13 in Supporting information). For erythritol, xylitol, D-mannitol/D-glucitol with DP of 4, 5 and 6, respectively, they are all crystalline. As reported by Yuan and coworkers [10], crystalline xylitol shows weak blue fluorescence with a QY of 1.5% and an RTP, but not a long phosphorescence lifetime even at a low temperature of 77 K. This suggests that polymerization can induce stronger TSI than crystallization to boost PL and RTP to some extent. Therefore, for amorphous PMO, there must be a critical DP (CDP) to achieve CL. However, owing to the polydispersity of polymers, it is difficult to synthesize monodisperse PMO. Here, we can't get the value of CDP experimentally, but it must exist. In fact, polymerization is only a prerequisite for the generation of oxygen clusters and TSI. Another factor that should be emphasized is H-bonding, which is the key to fluorescence and RTP, and the H-bonding strength must be strong enough. For example, for PVA with one less hydroxyl group in the building block, the very weak emission signal in the PL spectra and QY (Figs. S14 and S15 in Supporting information) is consistent with what we observed with the naked eye (Fig. 1). To some extent, H-bonding strength can be reflected by solubility and T_g. PVA is soluble in hot water and the highest T_g can reach up to 85 °C [53]. Compared to insoluble PMO with a T_g of 183.3 °C, the H-bonding strength of PVA is much lower than that of PMO. Therefore, only strong H-bonding can induce the through-space n-n interactions of oxygen atoms and further orbital splitting to achieve PL emission. In addition, strong H-bonding promotes conformational rigidification and significantly blocks nonradiative deactivation channels, conferring long-lived RTP emission. Like many traditional chromophores or PL materials without RTP, RTP appears once they are diffused into PVA or other polymers with strong H-bonding [34,54]. This work

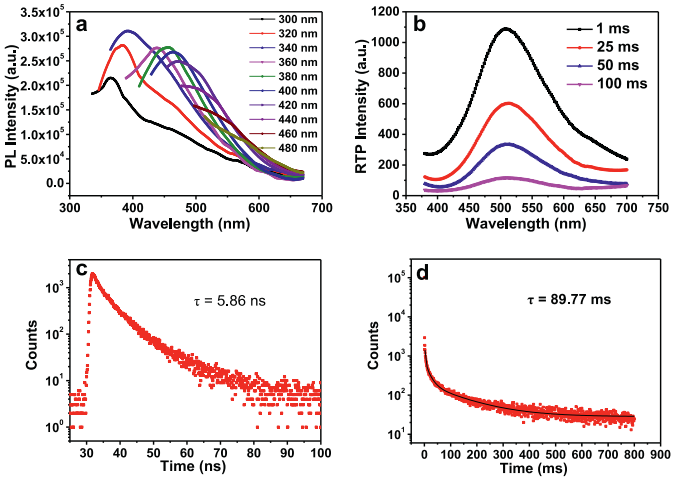

Fig. 3. (a) PL spectra of PBD at different excitation wavelengths in the solid state. (b) Time-resolved spectra of PBD at different delay times in the solid state (phosphorescence mode: λ_{ex} = 360 nm). (c) Luminescent and (d) phosphorescence decay curves of PBD in the solid state at 438 and 510 nm (λ_{ex} = 360 nm).

provides another avenue to understand the mechanism of PL and RTP.

The similar optical properties were observed in PBD with neighboring hydroxyl groups in the side chain (Fig. 3), confirming the significance of neighboring hydroxyl groups for fluorescence and RTP. As shown in Fig. 3a, it also exhibits excitation-dependent PL emission and emits the same emission peak at 438 nm excited by 360 nm. The RTP peak position and lifetimes of fluorescence and phosphorescence are close to those of PMO (Figs. 3b-d). Therefore, whether the neighboring hydroxyl groups are located in the backbone or side chain has no obvious effect on their luminescent properties. The strong intra-/intermolecular H-bonding interactions of PBD also results in insolubility in most solvents. In other words, when monomers with adjacent hydroxyl groups are polymerized, strong H-bonding can induce physical crosslinking, exhibiting strong intra-/intermolecular interactions. It is further demonstrated the TSI between the oxygen atoms.

To further fully confirm that the fluorescence and RTP originate from H-bonding induced through-space n-n interaction of oxygen atoms in oxygen clusters, the optimized conformations of PMO, PBD and PVA based on single polymer chains with fourteen

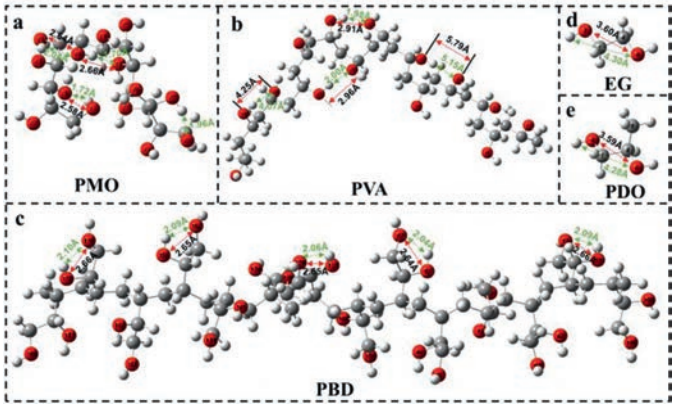

Fig. 4. Optimized conformations of (a) PMO, (b) PVA and (c) PBD based on single polymer chains with fourteen constitutional units at (DFT) B3LYP/6–31(d,p) level. Optimized conformations of (d) ethylene glycol and (e) 1,2-propanediol at (DFT) B3LYP/6–31(d,p) level. The red arrows represent the distance between oxygen atoms, and the green arrows represent the distance of H-bonding.

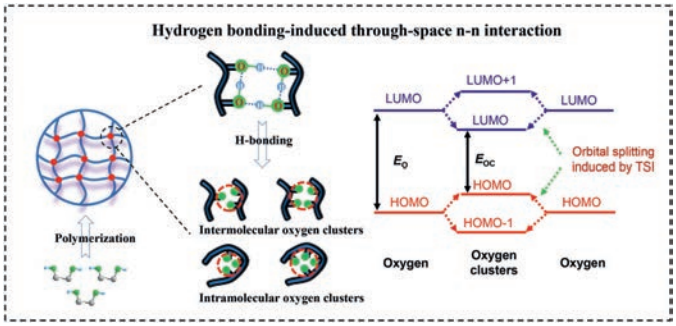

Fig. 5. A schematic diagram of TSI for PMO and PBD, and the orbital splitting induced by TSI, where E_O is the energy gap of the oxygen and E_{OC} is the energy gap of the oxygen cluster.

constitutional units were calculated by density functional theory (DFT) at B3LYP/6–31(d,p) level (Figs. 4a-c). Ethylene glycol and 1,2-propanediol, as repeating building blocks of PMO and PBD, were selected as controls and optimized at the same level (Figs. 4d and e). Fig. 4 shows that the presence of many short-range O···H in PMO and PBD, and some even below 1.72 Å, indicating strong H-bonding interactions [55]. Correspondingly, influenced by the H-bonding, intramolecular oxygen atoms aggregate to form oxygen clusters, and the distance between most of the oxygen atoms in PMO and PBD is 2.58−2.83 Å (Figs. 4a and c, Tables S1 and S2 in Supporting information), which is less than twice the van der Waals radius of the oxygen atom (d_O) (r_B: 1.52 Å; r_P: 1.40 Å). But for PVA, only two short-range O···H exist at the bending site, and the rest are all larger than 4.00 Å, far from the distance of H-bonding. This results in most of the oxygen atoms having a distance greater than d_O (Fig. 4b and Table S3 in Supporting information) and no oxygen clusters are produced. Furthermore, for ethylene glycol and 1,2-propanediol, the distance between adjacent hydroxyl groups is about 3.6 Å (Figs. 4d and e), which is much larger than d_O. Indeed, no fluorescence was detected in ethylene glycol (Fig. S12) and 1,2-propanediol (Fig. S16 in Supporting information). The importance of polymerization for TSI is well demonstrated. The above results fully confirm that the fluorescence and RTP of PMO and PBD are ascribed to the through-space n-n interaction between oxygen atoms induced by the strong H-bonding. In this case, the overlap of electron clouds of oxygen atoms leads to the splitting and coupling of the orbitals and the generation of new molecular orbitals with smaller energy gaps for visible light emission (Fig. 5). The resulting molecular orbitals correspond to the blue visible light of PMO and PBD. Owing to the difference in the distance between the oxygen atoms, the degree of electron cloud overlap and TSI is also different. As a consequence, it results in the generation of molecular orbitals with different energy gaps and the emergence of excitation-dependent PL and RTP emission. That is, the excitation-dependent PL and RTP emission are attributed to diverse oxygen clusters with different conjugated degrees, as detailed schematic diagram is shown in Fig. 5.

In summary, a novel class of amorphous polyols with fluorescence and long-lived RTP properties was prepared. Experimental results and theoretical calculations prove that the through-space n-n interaction of oxygen atoms is the fundamental cause of fluorescence and RTP. Results from controls (ethylene glycol, 1,2-propanediol, and PVA) confirm that polymerization and H-bonding play key roles in the generation of oxygen clusters and TSI. The difficulty of studying the photophysical behavior of PMO and PBD in solution limits the in-depth understanding of through-space n-n interactions to a certain extent. Our ongoing efforts are to seek a soluble strong H-bonded NCLP and to develop NCLPs with better optical performance. This work not only provides a new strategy for the design and construction of fluorescence and RTP materials, but also sheds new light on the CL mechanism of NCLPs.

Declaration of competing interest

There are no conflicts to declare.

Acknowledgments

We gratefully acknowledge the financial support of the National Natural Science Foundation of China (No. 52003254), the Shanxi Scholarship Council of China (No. 2020–051), the Shanxi-Zheda Institute of Advanced Materials and Chemical Engineering (No. 2021SX-TD012), the Foundational Research Project of Shanxi Province (Nos. 20210302123164, 201901D211282, 201901D211283), the Science Foundation of North University of China (No. XJJ201925) and the MOE Key Laboratory of Macromolecular Synthesis and Functionalization, Zhejiang University (No. 2021MSF01).

Supplementary materials

Supplementary material associated with this article can be found, in the online version, at doi:10.1016/j.cclet.2022.07.027.

References

[1] H. Hu, F. Meier, D. Zhao, et al., Adv. Mater. 30 (2018) 1707621.
[2] B. Sui, Y. Li, B. Yang, Chin. Chem. Lett. 31 (2020) 1443–1447.
[3] S. Jiang, L. Meng, W. Ma, et al., Chin. Chem. Lett. 32 (2021) 1037–1040.
[4] P. Shieh, M.J. Hangauer, C.R. Bertozzi, J. Am. Chem. Soc. 134 (2012) 17428–17431.
[5] L. Wang, W. Du, Z. Hu, et al., Angew. Chem. Int. Ed. 58 (2019) 14026–14043.
[6] S. Chen, L. Yin, L. Liu, et al., Chin. Chem. Lett. 32 (2021) 3133–3136.
[7] C. Weng, N. Fan, T. Xu, et al., Chin. Chem. Lett. 31 (2020) 1490–1498.
[8] Z.S. Li, Q. Zeng, G. Yu, et al., Macromol. Rapid Commun. 29 (2008) 136–141.
[9] G. Feng, B. Liu, Acc. Chem. Res. 51 (2018) 1404–1414.
[10] Y. Wang, X. Bin, X. Chen, et al., Macromol. Rapid Commun. 39 (2018) 1800528.
[11] X. Chen, Z. He, F. Kausar, et al., Macromolecules 51 (2018) 9035–9042.
[12] B. Chu, H. Zhang, L. Hu, et al., Angew. Chem. Int. Ed. 61 (2022) e202114117.
[13] Y. Gong, Y. Tan, J. Mei, et al., Sci. China Chem. 56 (2013) 1178–1182.
[14] X. Zhou, W. Luo, H. Nie, et al., J. Mater. Chem. C 5 (2017) 4775–4779.
[15] C. Shang, N. Wei, H. Zhuo, et al., J. Mater. Chem. C 5 (2017) 8082–8090.
[16] C. Hu, Z. Guo, Y. Ru, et al., Macromol. Rapid Commun. 39 (2018) 1800035.
[17] B. Zhao, S. Yang, X. Yong, J. Deng, ACS Appl. Mater. Interfaces 13 (2021) 59320–59328.
[18] D. Wang, T. Imae, J. Am. Chem. Soc. 126 (2004) 13204–13205.
[19] M. Sun, C.Y. Hong, C.Y. Pan, J. Am. Chem. Soc. 134 (2012) 20581–20584.
[20] B. Liu, Y.L. Wang, W. Bai, et al., J. Mater. Chem. C 5 (2017) 4892–4898.
[21] Y. Feng, T. Bai, H. Yan, et al., Macromolecules 52 (2019) 3075–3082.
[22] S. Tang, T. Yang, Z. Zhao, et al., Chem. Soc. Rev. 50 (2021) 12616–12655.

[23] H. Zhang, B.Z. Tang, JACS Au 1 (2021) 1805–1814.
[24] Q. Zhou, B. Cao, C. Zhu, et al., Small 12 (2016) 6586–6592.
[25] Q. Zhou, T. Yang, Z. Zhong, et al., Chem. Sci. 11 (2020) 2926–2933.
[26] Q. Wen, Q. Cai, P. Fu, et al., Chin. Chem. Lett. (2022), doi:10.1016/j.cclet.2022.06.015.
[27] B. Wang, H. Lin, J. Xu, et al., Inorg. Chem. 54 (2015) 11299–11306.
[28] M. Schulze, A. Steffen, F. Würthner, Angew. Chem. Int. Ed. 54 (2015) 1570–1573.
[29] M.S. Kwon, Y. Yu, C. Coburn, et al., Nat. Commun. 6 (2015) 8947.
[30] W. Luo, Y. Zhang, Y. Gong, et al., Chin. Chem. Lett. 29 (2018) 1533–1536.
[31] K. Narushima, Y. Kiyota, T. Mori, et al., Adv. Mater. 31 (2019) 1807268.
[32] G. Qu, Y. Zhang, X. Ma, Chin. Chem. Lett. 30 (2019) 1809–1814.
[33] X. Chen, W. Luo, H. Ma, et al., Sci. China Chem. 61 (2018) 351–359.
[34] M.S. Kwon, D. Lee, S. Seo, et al., Angew. Chem. Int. Ed. 53 (2014) 11177–11181.
[35] N.D. Field, J.R. Schaefgen, J. Polym. Sci. 58 (1962) 533–543.
[36] H.K. Reimschuessel, W.S. Creasy, J. Polym. Sci. Polym. Chem. Ed. 16 (1978) 845–860.
[37] D.C. Webster, Prog. Org. Coat. 47 (2003) 77–86.
[38] C. Unruh, D. Smith, J. Org. Chem. 23 (1958) 625-625.
[39] B. Kumru, N. Bicak, RSC Adv. 5 (2015) 30936–30942.
[40] K. Hayashi, G. Smets, J. Polym. Sci. 27 (1958) 275–283.
[41] L. Yuan, H. Yan, L. Bai, et al., Macromol. Rapid Commun. 40 (2019) 1800658.
[42] Z. Zhao, Y. Li, X. Chen, et al., Chem. Commun. 58 (2022) 545–548.
[43] J. Deng, H. Jia, W. Xie, et al., Macromol. Chem. Phys. 223 (2022) 2100425.
[44] B. Milián-Medina, J. Gierschner, WIREs Comput. Mol. Sci. 2 (2012) 513–524.
[45] D. Bhattacharyya, C. Elles, S. Bradforth, J. Phys. Chem. A (2019) 123.
[46] J. Liu, H. Zhang, L. Hu, et al., J. Am. Chem. Soc. 144 (2022) 7901–7910.
[47] J. Yang, X. Zhen, B. Wang, et al., Nat. Commun. 9 (2018) 840.
[48] Y. Liu, G. Zhan, Z.W. Liu, et al., Chin. Chem. Lett. 27 (2016) 1231–1240.
[49] B. Liu, H. Zhang, S. Liu, et al., Mater. Horiz. 7 (2020) 987–998.
[50] Y.N. Jing, S.S. Li, M. Su, et al., J. Am. Chem. Soc. 141 (2019) 16839–16848.
[51] S.S. Li, Y.N. Jing, H. Bao, et al., Cell Rep. Phys. Sci. 1 (2020) 100116.
[52] S.S. Li, N. Zhu, Y.N. Jing, et al., iScience 23 (2020) 101031.
[53] J.S. Park, J.-.W. Park, E. Ruckenstein, J. Appl. Polym. Sci. 82 (2001) 1816–1823.
[54] H. Wu, W. Chi, Z. Chen, et al., Adv. Funct. Mater. 29 (2019) 1807243.
[55] J.A. Erickson, J.I. McLoughlin, J. Org. Chem. 60 (1995) 1626–1631.